δ¹³C values in stalagmites from tropical South America for the last two millennia

Valdir Felipe Novello[1]*; Francisco William da Cruz[1], Mathias Vuille[2], José Leandro Pereira Silveira Campos[1], Nicolás Misailidis Stríkis[3], James Apaéstegui[4], Jean Sebastien Moquet[5], Vitor Azevedo[1], Angela Ampuero[3], Giselle Utida[1], Xianfeng Wang[6], Gustavo Macedo Paula-Santos[7], Plinio Jaqueto[8], Luiz Carlos Ruiz Pessenda[9], Daniel O Breecker[10], Ivo Karmann[1]

[1]Institute of Geosciences, University of São Paulo, São Paulo, 05508-080, Brazil.
[2]Department of Atmospheric and Environmental Sciences, University at Albany, Albany, 2222, USA.
[3]Departamento de Geoquímica, Universidade Federal Fluminense, Niterói, 24020-141, Brazil.
[4]Instituto Geofísico del Perú, Lima, 15012, Peru.
[5]Institut des Sciences de la Terre d'Orléans, Orléans, 45100, France.
[6]Earth Observatory of Singapore, Nanyang Technological University, Jurong West, 639798, Singapore.
[7]Institute of geoscience Umiversity of Campinas, 13083-855.
[8]Instituto de Astronomia, Geofísica e Ciências Atmosféricas, University of São Paulo, São Paulo, 05508-090, Brazil
[9]Center for Nuclear Energy in Agriculture (CENA), University of São Paulo, São Paulo, 13416-000, Brazil.
[10]Jackson School of Geosciences, University of Texas, Austin, 2305, USA.

*Correspondence to: Valdir F. Novello (vfnovello@gmail.com).

Abstract

Due to the many factors controlling δ¹³C values in stalagmites, complicating their paleoclimatic and paleoenvironmental interpretation, most studies do not present δ¹³C values, but instead focus mainly on δ¹⁸O values. This is also the case for most cave studies from tropical South America, where many new δ¹⁸O stalagmite records covering the last millennia were recently published. Here, we test the influence of local hydroclimate, altitude, temperature and changing vegetation types on δ¹³C values in stalagmites, by employing a new dataset (named δ¹³C_2k_SA - Novello et al., 2020, https://doi.pangaea.de/10.1594/PANGAEA.919050) composed of published and unpublished carbon isotope records from various sites in tropical South America. Most locations were dominated by C_3 plants over the last two millennia and are characterized by speleothem δ¹³C values more depleted than -6 ‰. The main factors influencing δ¹³C values are associated with the local hydroclimate, followed by minor effects from temperature. Most of the isotopic records show a significant correlation between the δ¹³C and δ¹⁸O values, indicating a close relationship between local hydroclimate and atmospheric convective processes related to the South American Monsoon System.

Earth System
Science
Data
Discussions
Open Access

1 Introduction

Measurements of carbon isotope (δ^{13}C) ratios are essential for (paleo)environmental studies, such as those regarding the carbon cycle, past food consumption by pre-historic societies, paleo-vegetation

40   reconstructions, soil dynamics, aspects regarding animal migration and food consumption, etc. (Rayner et al., 1999; Calo and Cortés, 2009; Pansani et al., 2019; Novello et al., 2019). However, δ^{13}C values of speleothems are generally considered difficult to interpret and, in most cases, are not reported in isotopic studies based on speleothems. Studies from tropical South America, in particular, have almost completely neglected δ^{13}C values from stalagmites and instead relied solely on δ^{18}O values for reconstruction of the

45   South American Monsoon System (SAMS) (Reuter et al., 2009; Novello et al., 2012; 2016; 2018; Apaéstegui et al., 2014; 2018; Vuille et al., 2012; Kanner et al., 2013; Wang et al., 2017). Here we present a compilation of 25 δ^{13}C records (13 of them hitherto unpublished) from stalagmites collected at different sites throughout tropical South America and covering the last two millennia (referred to here as the δ^{13}C_2k_SA dataset) with aims to characterize the main factors controlling δ^{13}C variability in these

50   stalagmites and provide possible paleoclimate and paleoenvironmental reconstructions for the region.
In Section 2 we review the mechanisms that control the δ^{13}C values in the stalagmites and the related global and regional forcings. In Section 3 we present the data, the stalagmites and methods. In Section 4 we present the study sites and describe the environmental and climate characteristics that might affect the δ^{13}C values in the stalagmites from tropical South America. In Section 5 we show the results (data set) and in Section

55   6 we discuss the interpretations of the new records and their regional relationships. Additionally, using Principal Component Analysis (PCA), we propose a new hydrological and vegetation index for South America based on the δ^{13}C_2k_SA dataset.

2. Background

2.1 Main processes controlling δ^{13}C values in speleothems

60   The initial source of carbon for speleothems is the soil CO_2 and tree roots. It forms carbonic acid in contact with water, which dissolves cave host-rock (limestones or dolostones) according to the equation:

$$\text{Eq.} \quad CaCO_3 + H_2O + CO_2 \leftrightarrow Ca^{2+} + 2HCO_3^- \quad (1)$$
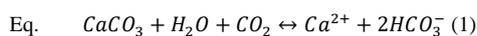
Open and closed system models were proposed to explain the dissolution of calcium carbonate in the percolating solution (Fohlmeister et al., 2011; McDermott et al., 2004, Hendy, 1971). Initially, the

65   percolating solution remains in equilibrium with the infinite reservoir of soil CO_2 and, thereby, the bicarbonate in solution receives its $\delta^{13}C$ fingerprint. Under these conditions, the contribution of the $\delta^{13}C$ values from the bedrock to the HCO_3^- in solution can be neglected. In a closed system, during the percolation into the epikarst, the solution loses contact with the soil CO_2, and the CO_2 in solution is progressively consumed through the dissolution of the bedrock. The rock dissolution is limited by the initial

70   amount of CO_2 and, consequently, through this process the $\delta^{13}C$ from the bedrock influences the isotopic composition of the remaining solution (McDermott, 2004). In most caves, the interaction between the percolation solution and the host-rock occurs as a partially open system. Thus, carbon in speleothems is sourced mainly from soil organic matter and tree roots, with a small proportion coming from the bedrock (usually less than 10%) (Genty et al., 2001).

75   The $\delta^{13}C$ values in pedogenic carbonate are closely related to the isotopic values from the surrounding vegetation (Cerling, 1984; Quade et al., 1989), defined by the plant type (C_3, C_4 or CAM), which in turn, will be conditioned by climatic parameters such as temperature, pluviosity, rainfall seasonality and atmospheric CO_2 (Ehleringer et al., 1997). Vegetation dominated by C_3 plants has $\delta^{13}C$ values between -32 ‰ and -20 ‰, while vegetation dominated by C_4 plants is characterized by values between -17 ‰ to -9 ‰

80   (Badeck et al., 2005). CAM plants have $\delta^{13}C$ values that overlap with both C_3 and C_4 plants. In addition, $\delta^{13}C$ values of individual C_3 plant species can vary approximately 1 to 2 ‰, depending on water availability (e.g., Hartman and Danin, 2010). The differences in the $\delta^{13}C$ values from total organic matter in soil resulting from the dominant plant types are transferred to stalagmites precipitated under their respective environment. Thus, stalagmites precipitated in caves under conditions dominated by C_3 plants typically

85   have values ranging from -14 ‰ to -6 ‰, while those forming below C_4 plant cover range from -6 % to +2 % (McDermott, 2004; Baker et al., 1997; Dreybrodt, 1988). Variations in soil $\delta^{13}C$ values and their evolution over time are controlled by carbon inputs from vegetation, which is proportional to the organic matter amount and vegetation density; thus denser vegetation is also associated with more depleted values in soil $\delta^{13}C$ and vice-versa (Pessenda et al., 2010). In addition, the $\delta^{13}C$ values of C_3 plants are sensitive to

90   atmospheric CO_2 levels (Van de Water et al., 1994; Schibert and Jahen 2012), producing a signal that is transferred to stalagmites (Breecker, 2017).

In the cave system, $\delta^{13}C$ values from dissolved inorganic carbon (DIC) can undergo fractionation through prior calcite precipitation (PCP), which preferentially removes ^{12}C from the solution during precipitation forced by CO_2 degassing (Micker et al., 2019), depleting ^{12}C from the final isotopic product recorded in

95   stalagmites (Baker et al., 1997). PCP increases during drier periods due to the increased exposure of seepage solution to air pockets along the epikarst flow routes, which results in CO_2 degassing from the solution, promoting the carbonate precipitation in the epikarst and/or stalactites (Fairchild and Baker, 2012). Therefore, PCP is climate related. In monsoonal climates, such as in (sub)tropical South America, the amount effect is the dominant process that affects the $\delta^{18}O$ value of rainwater, such that an increase in the

100   amount of rainfall results in waters with lower $\delta^{18}O$ values (Vuille et al., 2012). This increase in rainfall amount might also cause a decrease in the $\delta^{13}C$ value of speleothem calcite, by increasing the soil moisture content and soil respiration rates or by reducing PCP, resulting in a positive correlation between the $\delta^{18}O$ and $\delta^{13}C$ values of speleothem calcite/aragonite (Cruz et al., 2006; Mickler et al., 2006; and references therein). While $\delta^{13}C$ and $\delta^{18}O$ values may be correlated for different reasons, high correlation between both

105   isotopic ratios can also be indicative of forced kinetic fractionation, since carbon and oxygen are fractioned in the same direction in this process (Hendy et al., 1971). The isotopic disequilibrium increases with enhanced ventilation of the cave, which depends on temperature. However, the range of values resulting from the fractionation factor between $CaCO_3$ and HCO_3^- in tropical temperatures of $15 - 30$ °C has been documented to be < 0.5 ‰ (Polag et al., 2010 and references therein). Recently, Fohlmeister et al. (2020)

110   using a large dataset of $\delta^{13}C$ values in stalagmites deposited post-1900 CE show evidence for a temperature control on this proxy, likely driven by vegetation and soil processes, while PCP can explain the wide $\delta^{13}C$ range observed for concurrently deposited samples from the same cave.

2.2 Processes controlling the $\delta^{13}C$ values in speleothems from South America

The main mode of climate variability in tropical South America is defined by the SAMS behavior, which

115   also influences vegetation changes. Most of the $\delta^{18}O$ records from stalagmites in South America show a weak monsoon activity during the Medieval Climate Anomaly (MCA, 900-1100 years CE), in contrast with a strong activity during the Little Ice Age (LIA, 1600-1850 years CE) (Bird et al., 2011; Vuille et al., 2012; Novello et al., 2016; 2018). During the LIA period, a moisture dipole was documented between east and west portions of tropical South America, due to the displacement of the South Atlantic Convergence Zone

120   (SACZ) toward the southwest (Campos et al., 2019; Novello et al., 2018). The implications of this change

in climate on vegetation and local hydroclimate, which are parameters that heavily influence the $\delta^{13}C$ values in stalagmites, are still not well studied.

Few studies focused on the $\delta^{13}C$ values from speleothems in South America. Cruz et al. (2006) interpreted the $\delta^{13}C$ from Botuverá cave (southeastern Brazil) as a proxy for soil CO_2 productivity, which is modulated

125   at orbital time scales by changes in local temperature brought about by shifts between summer monsoonal and winter extratropical circulation. Novello et al. (2019) reported a decrease of 9 ‰ in the $\delta^{13}C$ values from Jaraguá cave (one of the caves of this study) during the transition between the last Glacial and the Holocene periods, resulting from a combination of changes above the cave, including: changes in the predominant vegetation type from C_4 to C_3, increase of organic matter and soil horizons, which were mainly

130   caused by the increase in temperature and atmospheric CO_2. For the last two millennia, Jaqueto et al. (2016) show that the concentration of magnetic minerals and $\delta^{13}C$ values in the ALHO6 stalagmite from Pau d'Alho cave is governed by soil dynamics and changes in vegetation cover above the cave. Dry periods are associated with less stable soils, resulting in high erosion and increased mineral flux into karst systems, which occurs simultaneously with increasing $\delta^{13}C$ values. Conversely, wetter periods with low $\delta^{13}C$ values

135   are associated with soils topped by denser vegetation that retains micrometer-scale pedogenic minerals and thus reduces detrital fluxes into the cave. Azevedo et al. (2019) further explored the relationship between $\delta^{13}C$ and $\delta^{18}O$ during the last millennium in a speleothem (MV3) from the Brazilian Central region, where wetter (drier) periods are also associated with lower (higher) values of $\delta^{18}O$ and $\delta^{13}C$ and higher (lower) speleothem growth rates. The same interpretation was utilized for the $\delta^{13}C$ values of the stalagmites from

140   Tamboril cave, located further south. However, at this site the $\delta^{18}O$ and $\delta^{13}C$ do not co-vary, which the authors interpret as a result of the decoupling between the local hydroclimate and SAMS, documented by the $\delta^{13}C$ and $\delta^{18}O$, respectively (Wortham et al., 2017).

The global increase of the atmospheric CO_2 concentration and temperature likely also influenced the $\delta^{13}C$ values of stalagmites during the last century. Since 1850 the land surface air temperature increased by about

145   1.44 °C (Jia et al., in press), affecting the fractionation between the seepage solution and the carbonate precipitated inside the caves (Lachniet, 2009), as well as promoting changes in cave ventilation (Baldini et al., 2008). Furthermore, depleted isotopic carbon has been emitted into the atmosphere due to the burning of fossil fuels, thereby decreasing the atmospheric $\delta^{13}C$ that is transferred to vegetation. The increase of atmospheric CO_2 can also favor the flourishing of C_3 plants, which are less adapted than C_4 plants to low

150   atmospheric CO_2 concentrations (Ehleringer et al., 1997).

3 Data Material and Methods

3.1 δ^{13}C data

The dataset used in this study comprises 25 speleothem δ^{13}C records, of which 13 were hitherto unpublished (Novello et al., 2020, available at https://doi.pangaea.de/10.1594/PANGAEA.919050). δ^{18}O records and

155   chronological models have been published for all stalagmite records. Data from the published records was obtained from the supplementary material of the respective papers or downloaded from the NOAA speleothem database (http://www.ncdc.noaa.gov/data-access/paleoclimatology-data/datasets/speleothem). Our main goal with this study is to introduce new cave records to the speleothem community and contextualize their interpretation in a regional framework for South America during the last two millennia.

160   For that, we used only datasets that were available to us with speleothem δ^{13}C data from the last two thousand years (since year 0 CE). Therefore, we only consider this time period for the analyses presented here. All records used, including their references, cave names, locations and climatic parameters, are listed in **Table 1**. They are composed of 11,601 δ^{13}C values from 25 speleothems, published in 15 different papers (**Table 1**).

165

Stalagmite	Cave	Latitude °N	Longitude °E	Reference	Annual Precipitation (mm)	Mean annual T (°C)	Elevation (m.a.s.l)
JAR4	Jaraguá	-21.08	-56.58	Novello et al. (2018; 2019) This study	1400	21.4	570
JAR1	Jaraguá	-21.08	-56.58	Novello et al. (2018) This study	1400	21.4	570
SBE3	São Bernardo	-13.81	-46.35	Novello et al. (2018) This study	1270	23.0	630
SMT5	São Matheus	-13.81	-46.35	Novello et al. (2018) This study	1270	23.0	630
ALHO6	Pau d'Alho	-15.21	-56.8	Novello et al. (2016) Jaqueto et al. (2016)	1440	25.5	340
CUR4	Curupira	-15.02	-56.78	Novello et al. (2016) This study	1440	25.5	340
DV2	Diva	-12.37	-41.57	Novello et al. (2012) This study	700	24.5	480
TR5	Torrinha	-12.37	-41.57	Novello et al. (2012) This study	700	24.5	480
LD12	Lapa Doce	-12.37	-41.57	Novello et al. (2012) This study	700	24.5	480
TRA7	Trapiá	-5.59	-37.70	Utida et al. (2020)	700	28.0	72
FN1	Furna Nova	-5.60	-37.44	Cruz et al. (2009) Utida et al. (2020)	700	28.0	100
TM0	Tamboril	-16.80	-47.27	Wortham et al. (2017)	1400	22.5	600
ANJOS1	Lapa dos Anjos	-14.39	-44.30	Stríkis (2015) This study	940	23.7	640
BTV21a	Botuverá	-27.21	-49.09	Bernal et al. (2016) This study	1400	22.0	200
PAR3	Paraiso	-4.07	-55.45	Wang et al. (2017)	2400	26.0	60
PAR1	Paraiso	-4.07	-55.45	Wang et al. (2017)	2400	26.0	60
MV3	Mata Virgem	-11.62	-47.49	Azevedo et al. (2019)	1570	26.8	365
POO-H1	Huagapo	-11.27	-75.79	Kanner et al. (2013)	459	10.4	3800
P09-H2	Huagapo	-11.27	-75.79	Kanner et al. (2013)	459	10.4	3800

BOTO3	Umajalanta–Chiflonkhakha	-18.12	-65.77	Apaéstegui et al. (2018) This study	518	17.0	2650
BOTO7	Umajalanta–Chiflonkhakha	-18.12	-65.77	Apaéstegui et al. (2018) This study	518	17.0	2650
BOTO10	Umajalanta–Chiflonkhakha	-18.12	-65.77	Apaéstegui et al. (2018) This study	518	17.0	2650
BOTO1	Umajalanta–Chiflonkhakha	-18.12	-65.77	Apaéstegui et al. (2018) This study	518	17.0	2650
PAL3	Palestina	-5.92	-77.35	Apaéstegui et al. (2014)	1570	22.8	870
PAL4	Palestina	-5.92	-77.35	Apaéstegui et al. (2014)	1570	22.8	870

Table 1: Caves, locations and regional characteristics.

3.2 Stalagmites

As presented in the original papers, all speleothems used in this study were collected with the initial goal

170   to reconstruct the SAMS using the $\delta^{18}O$ values. Therefore, stalagmites with a candle-type shape and uniform

growth were preferentially collected in isolated chambers located far from the cave entrance. At such

locations, temperature displays only minor variations throughout the year (characteristic of tropical caves),

the air circulation is restricted, CO_2 concentrations are higher than atmospheric values, and the air is

saturated in humidity. These conditions minimize the effects of ventilation, changes in temperature,

175   degassing and overall kinetic effects on the isotopic composition of the stalagmites.

3.3 Methods

To establish the correlation between the $\delta^{13}C$ and the growth rate from speleothems, we calculate the growth

rate based on the length of the interval between two consecutive U/Th ages and calculate the mean $\delta^{13}C$ for

the respective interval. For the correlation between the $\delta^{13}C$ values and local temperature and precipitation

180   we use a single average $\delta^{13}C$ value for each stalagmite, which was associated with the local mean

temperature and precipitation reported in the original papers.

In order to assess the shared variance among the $\delta^{13}C$ cave sites, while considering the stalagmites' age

uncertainties, we employ a Monte-Carlo Principal Component Analysis (MC-PCA), following the

methodology of Campos et al. (2019) and Deininger et al. (2017). The MC-PCA results in a set of loading

185   patterns representing the $\delta^{13}C$ spatial variability, and corresponding Principal Components, which

characterize the temporal variability of the loading patterns, each explaining a percentage of the shared

variance. 1000 Monte-Carlo simulations were performed using the isotopic time series obtained from the

interpolation of each individual stalagmite's age model. Isotopic records from the same cave or karst system

were merged in a single time series. To combine records, a normalization (z-score) of the shared period

190   using the mean and standard deviation of the longer time series was applied, before reconstructing the time

period through the inverse operation. This procedure resulted in a set of eight time series, each corresponding to a site shown in Fig. 1. Four stalagmites presented in Fig. 1 (MV3, FN1, TRA7, BTV21a) were not included in the PCA because these records do not cover the entire period of the last 2000 years and no other stalagmites from the same karst systems exist that could be merged, or because their data

195 resolution is significantly lower (more than 15 years between individual data points in the geochronological model). Given the time span covered by most records, the MC-PCA was evaluated only for the period from 650 to 1950 CE. To avoid biased results induced by large differences in altitude and temperature, linear regression analyses between the $\delta^{13}C$ data and temperature and altitude were performed excluding the sites from the high-altitude Andes (Umajalanta–Chiflonkhakha and Huagapo cave systems).

200 **4 Regional setting**

The speleothem $\delta^{13}C$ records used here are distributed throughout tropical South America (Fig. 1), covering a region spanning the latitudes 4 °S to 21 °S and longitudes 42 °W to 76 °W. The domain comprises the following climates (according to the Köppen climate classification): monsoon (Am), tropical savanna (Aw), warm semi-arid (BSh) and humid subtropical (Cwa). The annual precipitation amount ranges from 450 to

205 2400 mm, mainly related with the SAMS and its subcomponent the SACZ (Novello et al. 2018). The equatorial portion is also under direct influence of the Intertropical Convergence Zone (ITCZ). Except for the sites located in the Andes, all records are located at altitudes below 700 m.a.s.l. (**Table 1**). At these lowland sites, precipitation amount and the length of the rainy season define the three main vegetation types (Fig. 1). High precipitation amounts that are well distributed over the year are typical of Tropical Forest,

210 while Caatinga is characterized by an environment with lower precipitation, concentrated during a few months. Cerrado, the main biome of central South America, present hydrological conditions in-between these two end-members. In general, temperature decreases with increasing latitude and altitude; the mean annual temperature in the lowlands ranges from 21.4 to 26.8 °C, while the sites in the Andes reach temperatures around 10 °C (**Table 1**).
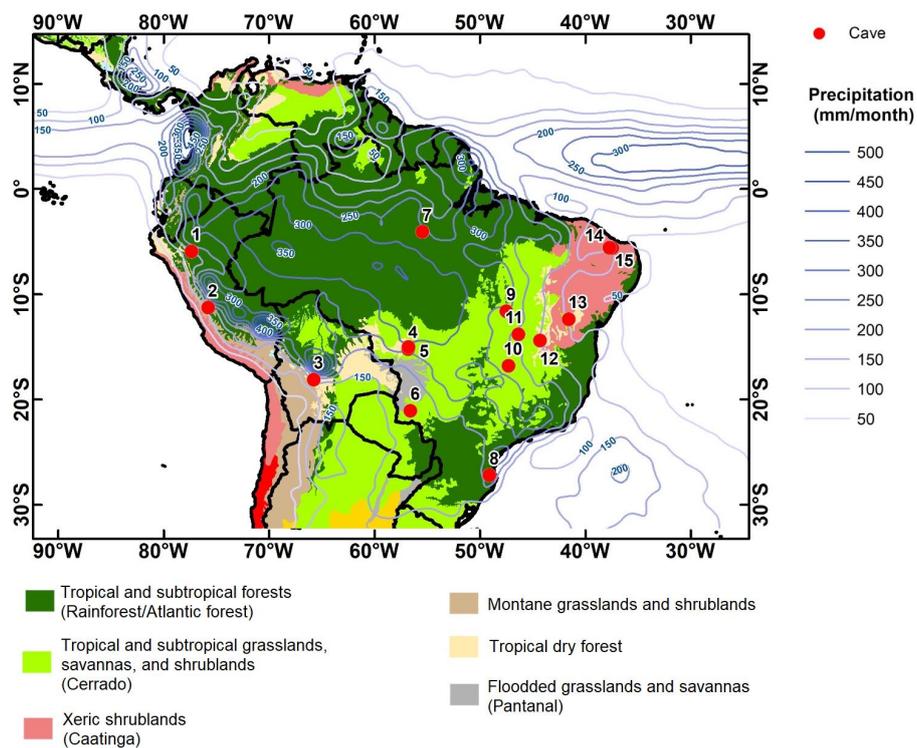
Figure 1: Map of tropical South America with vegetation types (Olson et al., 2001), the main biomes, precipitation (blue isolines - mm/month, derived from the annual mean for the period from 1998 to 2017, with data from TRMM 3b43 – Huffman et al., 2014) and location of the study sites from the δ^{13}C_2k_SA dataset. 1- Huagapo cave; 2- Palestina cave; 3- Umajalanta–Chiflonkhakha; 4- Pau d'Alho cave; 5- Curupira cave; 6- Járaguá cave; 7- Paraiso cave; 8- Botuverá cave; 9- Mata Virgem cave; 10- Tamboril cave; 11- São Matheus and São Bernardo cave system; 12- Anjos cave; 13- Diva, Torrinha, Lapa Doce caves; 14- Furna Nova cave; 15- Trapiá cave.

5 Results

The δ^{13}C values from the δ^{13}C_2k_SA dataset ranges from -11.5 to 6.8 ‰, although the large majority of the data lie within -11 and -1 ‰ (Appendix A, Fig. A1). The highest values and largest variability stem from the TR5 stalagmite, ranging from -3.8 to 6.8 ‰ (amplitude of 10 ‰), which contrasts with the average amplitude from the other stalagmites of 4.5 ‰. The vegetation domains of Tropical Forests (Rainforest/Atlantic forest) and Cerrado include the speleothems with the lowest δ^{13}C values (mean of -8.9 ‰ and -8.5 ‰, respectively), while the speleothems collected under the Caatinga domain have higher values (mean of -4.9 ‰) distributed over a large range (between 7.7 -4.9 ‰ and 3.1 ‰). High altitudes have the highest mean δ^{13}C values of ~ -3.5 ‰ (Appendix A, Fig. A2)

The coefficient of determination (R-square) between the $\delta^{18}O$ and $\delta^{13}C$ values of each stalagmite (Hendy test, Hendy et al., 1971) is shown in Appendix A, Table A1. The highest coefficient of determination (r^2: 0.96, p<0.01) is displayed by the TR5 stalagmite, while the average r^2 of the $\delta^{13}C\_2k\_SA$ dataset is 0.29. Average $\delta^{13}C$ values from the speleothems display a high negative correlation with the annual mean precipitation amount (r^2: 0.67, p < 0.01) and a weaker, positive correlation with temperature (r^2: 0.45, p<0.05) of their respective regions (Fig. 2). No significant correlation was found with altitude (p>0.05). The relationships between the growth rate and average $\delta^{13}C$ values are statistically significant (p≤0.05) only in the stalagmites JAR4 (r^2: 0.21), DV2 (r^2: 0.50), TR5 (r^2: 0.75), LD12 (r^2: 0.70) and TRA7 (r^2: 0.20), all with negative slopes (Appendix A, Table A2).
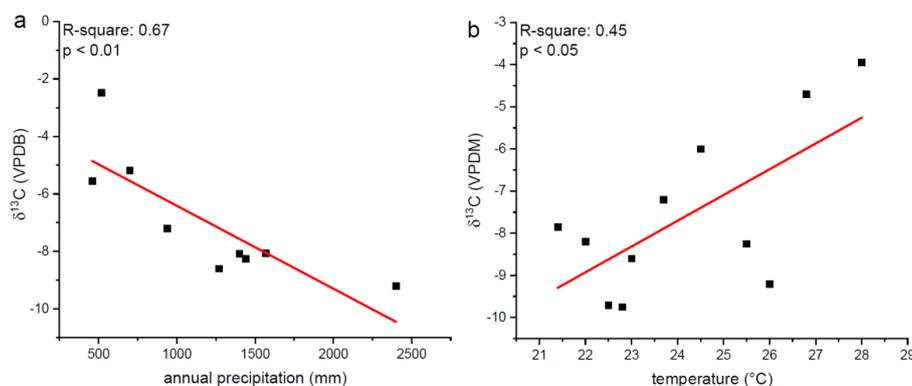

Figure 2: Relationship between the $\delta^{13}C$ from the $\delta^{13}C\_2k\_SA$ dataset with annual precipitation (a) and annual mean temperature (b) of each study site.

The MC-PCA methodology was applied to the full $\delta^{13}C\_2k\_SA$ dataset. The first principal component (PC1) explained ∼36 % of the total variance (Fig. 3 and 4). Positive loadings are associated with the $\delta^{13}C$ records from the caves Huagapo (Hua), Palestina (PAL), Jaraguá (Jar), and the merged records from the caves Pau d'Alho/Curupira (Alh) and São Bernardo/São Matheus (SBE), whereas negative loadings are linked to the records from the caves Diva de Maura/Torrinha/Lapa Doce (DV2), Paraiso caves (PAR) and Umajalanta–Chiflonkhakha (BOTO) (Fig. 3), indicating out of phase $\delta^{13}C$ variability between the two cave site groups. Positive values characterize the time interval of ∼600–1500 CE in PC1, while negative values are predominant during the period ∼1500–1950 CE, with an incursion to more negative values centered at ∼1180 CE (Fig. 4). PC2 explained ∼16 % of the variance, with large positive loadings displayed by the

records located in central Brazil, especially the TM0 and DV2 records, whereas large negative loadings are displayed by the records from high altitudes (PAL and BOTO). The other study sites present low and variable contributions for PC2. The temporal evolution of PC2 is characterized by predominantly positive values during the intervals 840-1110 CE and 1660-1950 CE, and negative values in the intervals 730-840

260   CE and 1110-1660 CE (Appendix A, Fig. A3).
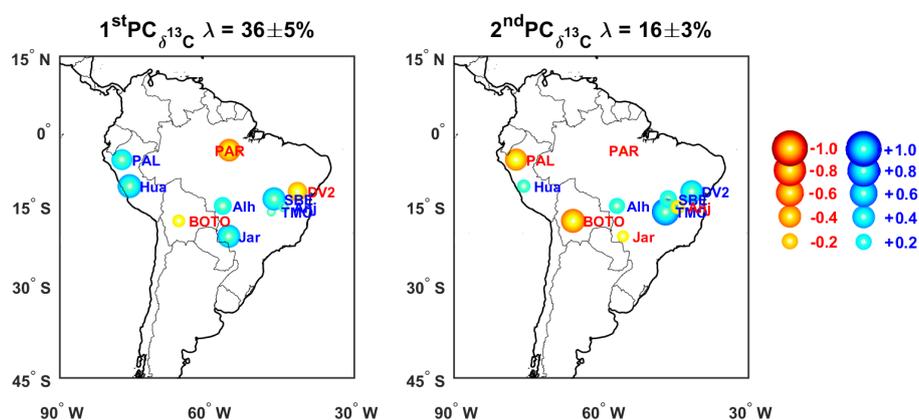
Figure 3: Maps of South America with the main loadings of the Principal Component Analysis (PCA) and explained total variance. Blue and red dots represent positive and negative loadings, respectively. The magnitude of the loadings is represented by the size of the dots. The larger the dot, the more representative it's loading is
265   **of the respective PC.**

6 Discussion

The host-rocks of the caves in this study are predominantly of Neoproterozoic age, located in the Brazilian shield (Appendix A, Table A1). Isotopic studies carried out in these carbonate rock sequences show a wide

270   range of values, varying between ~ -5 to 16 ‰ within the same rock unit or even the same outcrop (Appendix A, Table A1). The absence of isotopic studies in the same bedrock where the caves are located, precludes a precise quantification of the influence of these different rock sequences on the $\delta^{13}C$ values of the stalagmites. Of the study sites presented here, the $\delta^{13}C$ from its host-rock was only measured at Jaraguá and Trapiá caves (Novello et al., 2019; Utida et al., 2020). The dolomite of Jaraguá cave has $\delta^{13}C$ values of

275   ~1 ‰, which is similar to the values documented in the stalagmites of this cave growing during the last glacial period, in contrast to the low values (~-8.6 ‰) documented for stalagmites covering the Holocene period. Novello et al. (2019) associated the more depleted Holocene carbon isotopic values from this cave

with increased soil thickness, denser vegetation and the establishment of vegetation dominated by C_3 plants above the cave. The same interpretation was adopted for the $\delta^{13}C$ record from Trapiá cave, located in the

280 northeast of Brazil (Utida et al., 2020). At this site, however, the climate and environmental conditions were out of phase with Jaraguá Cave during the Holocene and glacial periods, and high $\delta^{13}C$ values in the stalagmites, similar to bedrock values (~0 ‰), were documented during the Holocene. In summary, both regions experienced a larger isotopic contribution from host rocks to the $\delta^{13}C$ values of their stalagmites during periods of sparse vegetation and thin soil layers above the caves. Indeed, nowadays these are the

285 typical characteristics of the sites Huagapo, Umajalanta–Chiflonkhakha, Mata Virgem, Trapiá and Torrinha; all featuring stalagmites with high $\delta^{13}C$ values (Appendix A, Fig. A1 and Table A1), these sites are also located in elevated altitudes or under Caatinga domain. Aside from the stalagmites of these sites and ALHO6, all other stalagmites have $\delta^{13}C$ values lower than -6 ‰, indicating the predominance of thick soil with higher organic matter content from the regions of Cerrado and/or Tropical Forest, sourced from

290 vegetation formed by C_3 plants over the last 2000 years.

TR5 presents $\delta^{13}C$ values that are significantly higher than all other samples, and the abrupt increase in $\delta^{13}C$ occurs just before the complete stop of carbonate deposition at ~1920 CE and ~2006 CE (Appendix A, Fig. A1), both of which are periods of predominantly dry conditions in the region (Novello et al., 2012). High values followed by an abrupt decrease also occur after the depositional hiatus at ~1960 CE. The r^2 between

295 $\delta^{13}C$ and $\delta^{18}O$ is close to 1 (Appendix A, Table A1), which indicates that both isotopes underwent fractionation together in this sample. These results support the notion that the TR5 stalagmite was precipitated under strong kinetic effects due to high evaporation rates and/or significantly reduced dripping rates (long time for isotope re-equilibration between solution and cave atmosphere) at the moment of carbonate precipitation, which is accentuated during drier periods, culminating in a complete halt of

300 carbonate precipitation. Although the kinetic effect might be the main factor responsible for the high amplitude and isotopic values in TR5, this stalagmite still preserves paleoclimate information regarding the $\delta^{18}O$ in precipitation that co-varies with the $\delta^{18}O$ from other stalagmites in the region, as well as with pluviometric data from meteorological stations (Novello et al., 2012).

Most of the stalagmites from the $\delta^{13}C\_2k\_SA$ dataset feature coefficients of determination between their

305 $\delta^{13}C$ and $\delta^{18}O$ values ranging from 0.20 to 0.56 (Appendix A, Table A1). The $\delta^{18}O$ values in stalagmites from tropical South America covering the last 2000 years has been interpreted as a proxy of the SAMS (Azevedo et al., 2019; Novello et al., 2012, 2016, 2018; Apaéstegui et al., 2014; 2018; Wortham et al.,

2017; Vuille et al., 2012) and the SACZ, a continuous band of low-level wind convergence and precipitation that extends in a northwest-southeast direction across southeastern South America (Novello et al., 2018).

310   Since an increase in local rainfall promotes a decrease of PCP, an increase in the production of soil organic matter and favors C_3 plants over C_4 plants (all processes that result in low $\delta^{13}C$ values in stalagmites), we argue that a correlation between $\delta^{13}C$ and $\delta^{18}O$ values is the result of a close relationship between local hydroclimate and atmospheric convective processes (inferred by $\delta^{18}O$). This hypothesis is supported by the existing correlation between the annual rainfall amount and the average $\delta^{13}C$ values of the stalagmites (r^2:

315   0.67, Fig. 2), and by the PC1 loadings derived from the $\delta^{13}C\_2k\_SA$ dataset (Fig. 3a), showing a very similar spatial distribution as those displayed in PC1 derived from the $\delta^{18}O$ dataset from speleothems over tropical South America by Campos et al. (2019). Both PC1-$\delta^{13}C$ and PC1-$\delta^{18}O$ show positive loadings for the locations to the southwest of the SACZ and negatives loadings for those records located to the northeast (Fig. 3), which characterizes the SACZ precipitation dipole in South America (Campos et al., 2019; Novello

320   et al., 2018). The BOTO site (Fig. 3) is an exception in this scenario, but this region have partially being under the influence from a different climate system with a different moisture source in the past (Apaéstegui et al., 2018). This relationship between the $\delta^{13}C$ and local hydroclimate was already documented for the ALHO6 stalagmite using a multiproxy approach (Jaqueto et al., 2016).
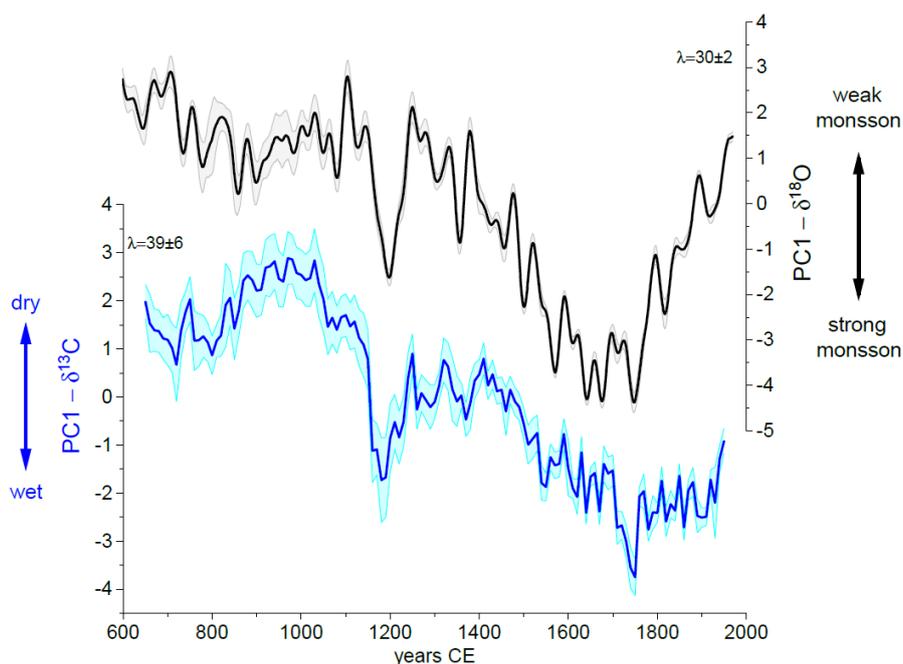
Figure 4: Comparison between the first Principal component (PC1) derived from the δ¹³C_2k dataset (this study) representing the main mode of hydroclimate variability and PC1 based on the δ¹⁸O from stalagmites from South America (PC1 – δ¹⁸O) from Campos et al. (2019) representing the main mode of variability of the South American Monsoon System. The error propagation from the PC1s are show by colored outlines. λ indicates the fraction of explained variance by each PC.

Strong correspondence throughout the time-series between scores of PC1-δ^{13}C and PC1-δ^{18}O further corroborates the overall coupling between the monsoon and local hydroclimate during the last ~1400 years (Fig. 4). This coupling ceases after ~1750 CE, when the monsoon weakened at a faster rate than the local hydrological response. However, the hydrologic variability inferred from PC1-δ^{13}C is biased by vegetation changes, which responds to other influences beyond the local rainfall amount, such as temperature and atmospheric CO_2 (both of which are parameters that have increased significantly over the last 200 years).

PC2 explains only 16 % of the δ^{13}C variability (Fig. 3, Appendix A, Fig. A3). It shows large positive loadings at sites located in lowlands of central Brazil and negative loadings at sites located at the Andes (Fig. 3). Since the δ^{13}C_SA_2k dataset is significantly influenced by temperature (Fig. 2b), the small contribution of PC2 to the δ^{13}C_SA_2k dataset may be related to different effects of temperature at different altitudes. Changes in continental temperature are amplified at higher elevation (Ohmura, 2012), leading to

14

a larger effect on the $\delta^{13}C$ values at sites located at higher altitudes, thereby increasing the isotopic differences between sites located at low and high elevation.

345   Growth rates also show a weak correlation with the $\delta^{13}C$ values from the $\delta^{13}C\_2k\_SA$ dataset. The correlation between the growth rate and $\delta^{13}C$ values is statistically significant (p-values ≤ 0.05) only in the stalagmites JAR4, DV2, TR5, LD12 and TRA7. In these stalagmites, all regression coefficients present a negative slope, which is expected, as a higher growth rate leads to lower $\delta^{13}C$ values because the time for isotopic enrichment of the DIC through kinetic effects is reduced during carbonate precipitation 350   (Fohlmeister et al., 2020).

7 Conclusions

Here we present a new set of $\delta^{13}C$ records from speleothems collected over a broad region of tropical South America. These data were integrated with previously published speleothem $\delta^{13}C$ records to characterize the main controls on carbon isotope variations in this region. The predominance of C_3 plants above most of the 355   karst systems studies here is responsible for the low $\delta^{13}C$ values (< -6 ‰) in most of the speleothems, while local hydroclimate is the main driver behind its variability during the last two millennia. Unlike what was observed in the global compilation of $\delta^{13}C$ records for the period after 1900 CE (Fohlmeister et al., 2020), local temperature and growth rate play a minor role in the shaping the $\delta^{13}C$ values in the $\delta^{13}C\_2k\_SA$ dataset. The probable reason for this difference between studies is that most of the speleothems in our 360   database formed under tropical conditions, characterized by a limited temperature range, whereas the SISAL_v1 dataset studied by Fohlmeister et al. (2020) is biased towards records from high latitudes with a much large temperature range.

Using Monte Carlo Principal Component Analysis, we produce an index of the mean hydrologic conditions and its changes over tropical South America for the last two millennia, which is closely related to monsoon 365   variability for the period prior to 1750 CE. The recent break-down in the relationship between monsoon and local hydroclimate may have been caused by the increase in temperature and CO_2 during the current warm period; however, further studies are required to test this hypothesis.

8 Data availability

The new $\delta^{13}C$ records from $\delta^{13}C\_2k\_SA$ dataset can be found in Novello et al. (2020) available at 370   PANGAEA: (https://doi.pangaea.de/10.1594/PANGAEA.919050.

References

Alvarenga, C. J. S., Santos, R. V., Vieira, L. C., Lima, Barbara, A. F. and Mancini, L. H.: Meso-Neoproterozoic isotope stratigraphy on carbonates platforms in the Brasilia Belt of Brazil. Precambrian. Res., 251, 164-180, doi.org/10.1016/j.precamres.2014.06.011, 2014.

375 Apaéstegui, J., Cruz, F. W., Vuille, M., Fohlmeister, J., Espinoza, J. C., Sifeddine, A., Strikis, N., Guyot, J. L., Ventura, R., Cheng, H. and Edwards, R. L.: Precipitation changes over the eastern Bolivian Andes inferred from speleothem (d18O) records for the last 1400 years. Earth Planet. Sci. Lett., 494, 124 – 134, doi.org/10.1016/j.epsl.2018.04.048, 2018.

Apaéstegui, J., Cruz, F. W., Sifeddine, A., Vuille, M., Espinoza, J. C., Guyot, J.-L., Khodri, M., Strikis, N., 380 Santos, R. V., Cheng, H., Edwards, L., Carvalho, E. and Santini, W.: Hydroclimate variability of the northwestern Amazon Basin near the Andean foothills of Peru related to the South American Monsoon System during the last 1600 years. Clim. Past, 10, 1967–1981, doi.org/10.5194/cp-10-1967-2014, 2014.

Azevedo, V., Stríkis, N. M., Santos, R. A., Souza, J. G., Ampuero, A., Cruz, F. W., Oliveira, P., Stumpf, 385 C. F., Vuille, M., Mendes, V. R., Cheng, H. and Edwards, R. L.: Medieval Climate Variability in the eastern Amazon-Cerrado regions and its archeological implications. Sci. Rep., 9, 20306, doi:.org/10.1038/s41598-019-56852-7, 2019.

Badeck, F. W., Tcherkez, G., Nogues, S., Piel, C. and Ghashghaie, J.: Post-photosynthetic fractionation of stable carbon isotopes between plant organs—a widespread phenomenon. Rapid. Commun. Mass 390 Sp., 19(11), 1381-1391, 2005.

Baker, A., Ito, E., Smart, P.L. and McEwan, R.F.: Elevated and variable values of d13C in speleothems in a British cave system. Chem. Geol., 136, 263–270, 1997.

Baldini, J. U. L., McDermott, F., Hoffmann, D. L., Richards, D. A. and Clipson, N.: Very high-frequency and seasonal cave atmosphere PCO2 variability: implications for stalagmite growth and oxygen 395 isotope-based paleoclimate records. Earth Planet Sci. Lett., 272, 118–129, 2008.

Bernal, J. P., Cruz, F. W., Stríkis, N. M., Wang, X., Deininger, M., Catunda, M. C. A., Ortega-Obregón, C., Cheng, H., Edwards, R. L., Auler, A. S.: High-resolution Holocene South American monsoon

history recorded by a speleothem from Botuverá Cave, Brazil. Earth Planet. Sci. Lett., 450, 186-196, dx.doi.org/10.1016/j.epsl.2016.06.008, 2016.

400 Bird, B. W., Abbott, M. B., Vuille, M., Rodbell, D. T., Stansell, N. D. and Rosenmeier, M. F.: A 2,300-year-long annually resolved record of the South American summer monsoon from the Peruvian Andes. Proc. Natl. Acad. Sci., 108(21), 8583–8588, doi.org/10.1073/pnas.1003719108, 2011.

Breecker, D. O.: Atmospheric pCO2 control on speleothem stable carbon isotope compositions. Earth. Planet. Sci. Lett., 458, 58-68, 2017.

405 Caetano-Filho, S., Paula-Santos, G. M., Guacaneme, C., Babinski, M., Babinski, M., Bedoya-Rueda, C., Peloso, M., Amorim, K., Afonso, J., Kuchenbecker, M., Reis, H. L. S. and Trindade, R. I. F.: Sequence stratigraphy and chemostratigraphy of an Ediacaran-Cambrian foreland-related carbonate ramp (Bambuí Group, Brazil). Precambrian. Res., 331, 105365. doi.org/10.1016/j.precamres.2019.105365, 2019.

410 Caird, R. A., Pufahl, P. K., Hiatt, E. E., Abram, M. B., Rocha, A. J. D. and Kyser, T. K.: Ediacaran stromatolites and intertidal phosphorite of the Salitre Formation, Brazil: Phosphogenesis during the Neoproterozoic Oxygenation Event. Sediment. Geol., 350, 55-71. doi,org/10.1016/j.sedgeo.2017.01.005, 2017.

Calo, C. M. and Cortés, L. I.: A contribution to the study of diet of formative societies in Northwestern
415 Argentina: isotopic and archaeological evidence. Int. J. Osteoarchaeol., 19, 192-203, doi:10.1002/oa.1052, 2009.

Campos, A. C. P. P.: Paleoambiente e quimioestratigrafia da formação Itaituba, carbonífero da borda sul da Bacia do Amazonas, região de Uruará – Pará. Amélia Carolina Pimenta Parente de Campos. M. S. thesis, Universidade Federal do Pará, Brazil, 77 pp, 2013.

420 Campos, J. L. P. S., Cruz, F. W., Ambrizzi, T., Deininger, M., Vuille, M., Novello, V. F. and Stríkis, N. M.: Coherent South American monsoon variability during the last millennium revealed through high-resolution proxy records, Geophys. Res. Lett., 46, doi.org/10.1029/2019GL0825132019, 2019.

Cerling, T. E.: The stable isotopic composition of modern soil carbonate and its relationship to climate. Earth. Planet. Sci. Lett., 71(2), 229-240, 1984.

425   Cruz, F. W., Burns, S. J., Jercinovic, M., Karmann, I., Sharp, W. D. and Vuille, M.: Evidence of rainfall
           variations in Southern Brazil from trace element ratios (Mg/Ca and Sr/Ca) in a Late Pleistocene
           stalagmite. Earth Planet Sci. Lett., 71, 2250-2263, doi:10.1016/j.gca.2007.02.005, 2006.

       Cruz, F. W., Vuille, M., Burns, S. J., Wang, X., Cheng, H., Werner, M., Edwards, R. L., Karmann, I., Auler,
           A. S. and Nguyen, H.: Orbitally driven east-west antiphasing of South American precipitation. Nat.
430   Geosc., 2, 210-214, doi:10.1038/NGEO0444, 2009.

       Deininger, M., McDermott, F., Mudelsee, M., Werner, M., Frank, N. and Mangini, A.: Coherency of late
           Holocene European speleothem $\delta 18O$ records linked to North Atlantic Ocean circulation. Climate
           Dynamics, 49 (1-2), 595–618, doi.org/10.1007/s00382-016-3360-8, 2017.

       Dreybrodt, W.: Processes in Karst Systems. Springer Series in Physical Environment. Springer, Heidelberg,
435   282pp, 1988.

       Ehleringer, J. R., Cerling, T. E. and Helliker, B. R.: C_4 photosynthesis, atmospheric CO_2, and climate.
           Oecologia, 112, 285-299, 1997.

       Fairchild, I. J., Baker, A. (Eds): Speleothem Science: From Process to Past Environments, Wiley-
           Blackwell, 2012.

440   Fohlmeister, J., Voarintsoa, N. R. G., Lechleitner, F. A., Boyd, M., Brandstätter, S., Jacobson, M. J. and
           Oster, J.: Main controls on the Stable Carbon Isotope Composition of Speleothems. Geochim.
           Cosmochim. Acta, GCA11710, 2020.

       Fohlmeister, J., Scholz, D., Kromer, B. and Mangini, A.: Modelling carbon isotopes of carbonates in cave
           drip water. Geochimica et Cosmochimica Acta, 75(18), 5219-5228, 2011.

445   Genty, D., Baker, A., Massault, M., Proctor, C., Gilmour, M., Pons-Branchu, E. and Hamelin, B.: Dead
           carbon in stalagmites: Carbonate bedrock paleodissolution vs. ageing of soil organic matter.
           Implications for ^{13}C variations in speleothems. Geochim. Cosmochim. Ac. 65, 3443-3457, 2001.

       Hartman G. and Danin A.: Isotopic values of plants in relation to water availability in the Eastern
           Mediterranean region. Oecologia 162, 837–852, 2010.

450   Hendy, C. H.: The isotopic geochemistry of speleothems 1. The calculation of the effects of the different
           modes of formation on the isotopic composition of speleothems and their applicability as
           palaeoclimatic indicators. Geochim. Cosmochim. Ac., 35, 801–824, 1971.

Huffman, G., Bolvin, D. T., Braithwaite, D., Hsu, K., Joyce, R., Xie, P.: Integrated Multi-satellitE Retrievals for GPM (IMERG), version 4.4. NASA's Precip. Process. Cent, 2014.

455   Jaqueto, P., Trindade, R. I. F., Hartmann, G. A., Novello, V. F., Cruz, F. W., Karmann, I, Strauss, B. E. and Feinberg, J. M.: Linking speleothem and soil magnetism in the Pau d'Alho cave (central South America). J. Geophys. Res. Solid. Earth, 121, doi:10.1002/2016JB013541, 2017.

Jia, G., E. Shevliakova, Artaxo P., De Noblet-Ducoudré, N., Houghton, R., House, J., Kitajima, K., Lennard, C., Popp, A., Sirin, A., Sukumar, R., Verchot, L.: Land–climate interactions. In: Climate
460   Change and Land: an IPCC special report on climate change, desertification, land degradation, sustainable land management, food security, and greenhouse gas fluxes in terrestrial ecosystems [Shukla, P.R., Skea, J., Calvo Buendia, E., Masson-Delmotte, V., Pörtner, H.-O., Roberts, D. C., Zhai, P., Slade, R., Connors, S., Van Diemen, Ferrat, R. M., Haughey, E., Luz, S., Neogi, S., Pathak, M., Petzold, J., Portugal Pereira, J., Vyas, P., Huntley, E., Kissick, K., Belkacemi, M., Malley, J. (eds.)].
465   In press.

Kanner, L. C., Burns, S. J., Cheng, H., Edwards, R. L. and Vuille, M.: High-resolution variability of the South American summer monsoon over the last seven millennia: insights from a speleothem record from the central Peruvian Andes. Quat. Sci. Rev., 75, 1-10, doi.org/10.1016/j.quascirev.2013.05.008, 2013.

470   Lachniet, M. S.: Climatic and environmental controls on speleothem oxygen-isotope values. Quat. Sci. Rev., 28, 412-432, 2009.

Lima, O. N. B.: Estratigrafia isotópica e evolução sedimentar do Grupo Bambuí na borda ocidental do Cráton do São Francisco: implicação tectônica e paleo-ambiental. Ph.D. thesis, Universidade de Brasilia, Brazil, 114 pp., 2011.

475   McDermott, F.: Palaeo-climate reconstruction from stable isotope variations in speleothems: a review. Quat. Sci. Rev., 23, 901–918, doi .org /10.1016 /j.quascirev.2003.06.021, 2004.

Meyer, K. W., Feng, W., Breecker, D. O., Banner, J. L. and Guilfoyle, A.: Interpretation of speleothem calcite $\delta^{13}C$ variations: Evidence from monitoring soil CO_2, drip water, and modern speleothem calcite in central Texas. Geochim. Cosmochim. Ac., 142, 281-298, 2014.

480   Mickler, P. J., Carlson, P., Banner, J. L., Breecker, D. O., Stern, L. and Guilfoyle, A.: Quantifying carbon
          isotope disequilibrium during in-cave evolution of drip water along discreet flow paths. Geochimica et
          Cosmochimica Acta, 244, 182-196, 2019.

       Mickler, P. J., Stern, L. A. and Banner, J. L.: Large Kinect isotope effects in modern speleothems. Geol.
          Soc. Am. Bull., 118, 65-81, doi.10.1130/B25698.1, 2006.

485   Nogueira, A. C. R. and Riccomini, C.: O Grupo Araras (Neoproterozóico) na parte norte da faixa Paraguai
          e sul do craton amazônico, Brasil. Braz. J. Geol., 36, 576-587, 2006.

       Novello, V. F., Azevedo, V., Apáestegui, J. and Wang, X.: δ^{13}C stalagmite records from South America.
          PANGAEA, https://doi.pangaea.de/10.1594/PANGAEA.919050.

       Novello, V. F., Cruz, F. W., Karmann, I., Burns, S. J., Stríkis, N. M., Vuille, M., Cheng, H., Edwards, R.
490   L., Santos, R. V., Frigo, E. and Barreto, E. A. S.: Multidecadal climate variability in Brazil's Nordeste
          during the last 3000 years based on speleothem isotope records. Geophys. Res, Lett., 39, L23706, doi:
          10.1029/2012GL053936, 2012.

       Novello, V. F., Vuille, M., Cruz, F. W., Stríkis, N. M., Saito de Paula, M., Edwards, R. L., Cheng, H.,
          Karmann, I., Jaqueto, P. F., Trindade, R. I. F., Hartmann, G. A. and Moquet, J. S.: Centennial-scale
495   solar forcing of the South American Monsoon System recorded in stalagmites. Sci. Rep., 6, 24762,
          doi:10.1038/srep24762, 2016.

       Novello, V. F., Cruz, F. W., Moquet, J. S., Vuille, M., de Paula, M. S.; Nunes, D., Edwards, R. L., Cheng,
          H., Karmann, I., Utida, G., Stríkis, N. M., Campos, J. L. P. S.: Two millennia of South Atlantic
          Convergence Zone variability reconstructed from isotopic proxies. Geophys. Res, Lett., 45,
500   doi.org/10.1029/2017GL076838, 2018.

       Novello, V. F., Cruz, F. W., McGlue, M. M., Wong, C. I., Ward, B. M., Vuille, M., Santos, R. A., Jaqueto,
          P., Pessenda, L. C. R., Atorre, T., Ribeiro, L. M. A. L., Karmann, I., Barreto, E. S.; Cheng, H., Edwards,
          R. L., Paula, M. S. and Scholz, D.: Vegetation and environmental changes in tropical South America
          from the last glacial to the Holocene documented by multiple cave sediment proxies. Earth Planet. Sci.
505   Lett., 524, 115717, doi.org/10.1016/j.epsl.2019.115717, 2019.

       Ohmura, A.: Enhanced temperature variability in high-altitude climate change. Theor. Appl. Climatol., 110,
          499-508, 2012.

Olson, D. M., Dinerstein, E., Wikramanayake, E. D., Burgess, N. D., Powell, G. V. N., Underwood, E. C., D'amico, J. A., Itoua, I., Strand, H. E., Morrison, J. C., Loucks, C. J., Allnut, T. F., Ricketts, T. H., Kura, Y., Lamoreus, J. F., Wettengel, W. W., Hedao, P., Kassem, K. R.: Terrestrial Ecoregions of the World: A New Map of Life on Earth. Bioscience, 51, 933-938, doi.org/10.1641/0006-3568(2001)051[0933:TEOTWA]2.0.CO;2, 2001.

Pansani, T. R., Muniz, F. P., Cherkinsky, A., Pacheco, M. L. A. F. and Dantas, M. A. T.: Isotopic paleoecology ($\delta^{13}C$, $\delta^{18}O$) of Late Quaternary megafauna from Mato Grosso do Sul and Bahia States, Brazil. Quat. Sci. Rev., 221, 105864, 2019.

Pessenda, L. C. R., Gouveia, S. E. M., Ribeiro, A. S., Oliveira, P. E. and Aravena, R.: Late Pleistocene and Holocene vegetation changes in northeastern Brazil determined from carbon isotopes and charcoal records in soil. Palaeogeogr. Palaeocl., 297, 597-608, doi:10.1016/j.palaeo.2010.09.008, 2010.

Polag, D., Scholz, D., Mühlinghaus, C., Spötl, C., Schröder-Ritzrau, A., Segl, M. and Mangini, A.: Stable isotope fractionation in speleothems: Laboratory experiments. Chem. Geol., 279, 31-39, 2010.

Quade, J., Cerling, T. E. and Bowman, J. R.: Systematic variations in the carbon and oxygen isotopic composition of pedogenic carbonate along transects in the Southern Great Basin, United States. Geol. Soc. Am. Bull., 101: 464-475, 1989.

Rayner, P. J., Enting, I. G., Francey, R. J. and Langenfelds, R.: Reconstructing the recent carbon cycle from atmospheric CO_2, $\delta^{13}C$ and O_2/N_2 observations. Tellus B, 51:2, 213-232, doi:10.3402/tellusb.v51i2.16273, 1999.

Reuter, J., Stott, L., Khider, D., Sinha, A., Cheng, H. and Edwards, R. L.: A new perspective on the hydroclimate variability in northern South America during the Little Ice Age. Geophys. Res, Lett., 36, L21706, doi:10.1029/2009GL041051, 2009.

Salomons, W. and Mook, W. G.: Isotope geochemistry of carbonates in the weathering zone. In: Fritz, P., Fontes, C.J. (Eds.), Handbook of Environmental Isotope Geochemistry, Vol. 2. The Terrestrial Environment, B. Elsevier, Amsterdam, 239–270 pp, 1986.

Schubert, B. A. and Jahren, A. H.: The effect of atmospheric CO_2 concentration on carbon isotope fractionation in C_3 land plants. Geochim. Cosmochim. Ac., 96, 29-43, 2012.

535   Strikís, N. M.: Atividade do Sistema de Monção Sul-americana na porção central do Brasil durante o último período glacial a partir da aplicação de isótopos de oxigênio em espeleotemas, Ph.D. thesis, Instituto de Geociências, Universidade de São Paulo, Brazil, 265 pp., 2015.

Utida, G., Cruz, F. W., Santos, R. V., Sawakuchi, A. O., Wang, H., Pessenda, L. C. R., Novello, V. F., Vuille, M., Stríkis, N. M., Guedes, C., Cheng, H., Edwards, R. L.: Climate changes in Northeastern
540   Brazil from Deglacial to Meghalayan periods and related environmental impacts. Quat. Sci. Rev., submitted, 2020.

Van de Water, P. K., Leavitt, S. W. and Betancourt, J. L.: Trends in stomatal density and 13C/12C ratios of Pinus flexilis needles during last glacial-interglacial cycle. Science, 264(5156), 239-243, 1994.

Vuille, M., Burns, S. J., Taylor, B. L., Cruz, F. W., Bird, B. W., Abbott, M. B., Kanner, L. C., Cheng, H. and Novello, V. F.: A review of the South American Monsoon history as recorded in stable isotopic
545   proxies over the past two millennia. Clim. Past, 8(4), 1309–1321, doi.org/10.5194/cp-8-1309-2012, 2012.

Wang, X., Edwards, R. L., Auler, A. S., Cheng, H., Kong, X., Wang, Y., Cruz, F. W., Dorale, J. A. D. and Chiang, H.-W.: Hydroclimate changes across the Amazon lowlands over the past 45,000 years. Nature,
550   541, 204 – 209. doi:10.1038/nature20787, 2017.

Wortham, B. E., Wong, C. I., Silva, L. C. R., McGee, D., Montañez, I. P., Rasbury, E. T., Cooper, K. M., Sharp, W. D., Glessner, J. J. G. and Santos, R. V.: Assessing response of local moisture conditions in central Brazil to variability in regional monsoon intensity using speleothem [87]Sr/[86]Sr values. Earth. Planet. Sci. Lett., 463, 310-322, doi.org/10.1016/j.epsl.2017.01.034, 2017.

555

560

Competing interests: The authors declare that they have no conflict of interest.

570

575

580

585

Appendix A
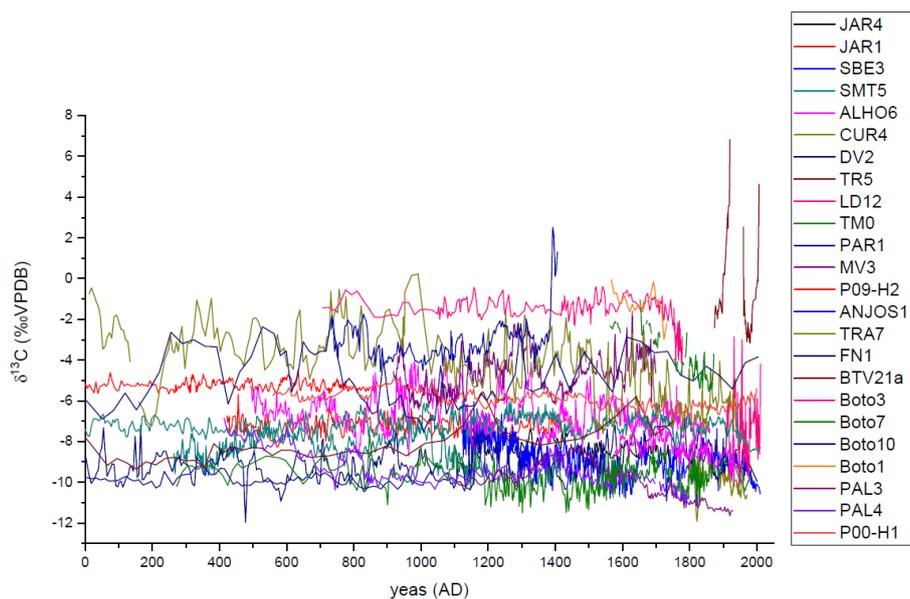
**Figure A1: δ¹³C records of stalagmites from tropical South America.**

590
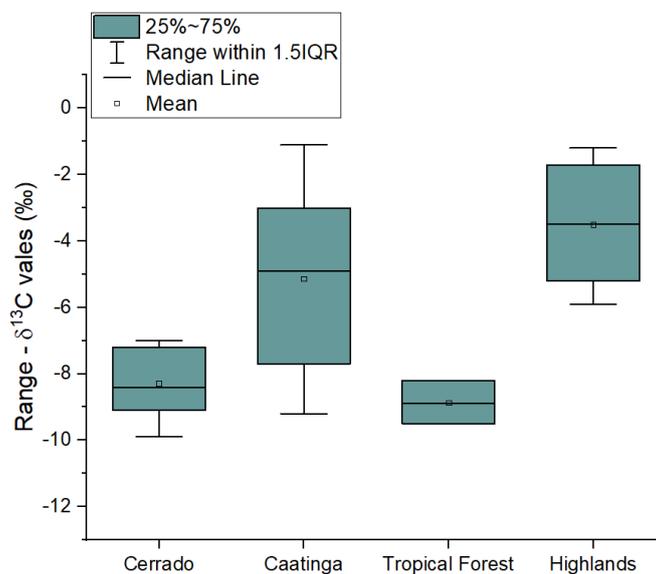
Figure A2: Box plot with means of the δ¹³C values of stalagmites from each vegetation domain.
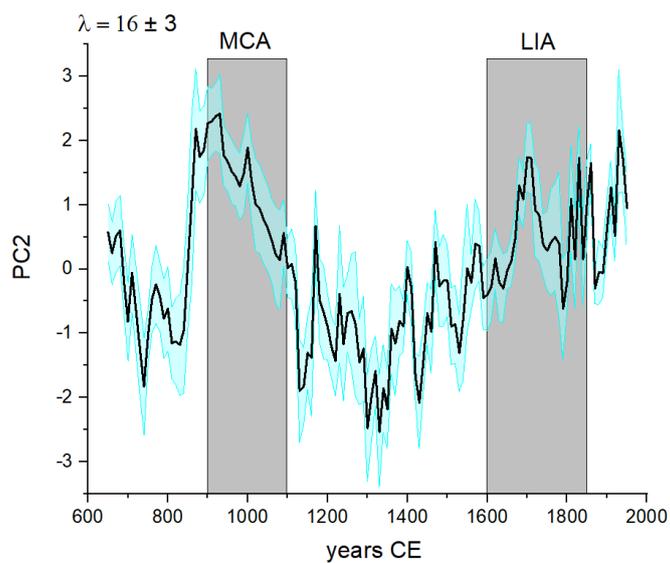
Figure A3: PC2 derived from the δ¹³C_2k dataset, explaining 16±3 % of the total variance.

595

600

Stalagmite	δ¹⁸O mean	δ¹³C mean	R-square δ¹⁸O x δ¹³C	Time period covered (years BP)	Isotopic data points	Mean resolution (years)	δ¹³C of the main rock formation	Host geology
JAR4	-4.8	-8.5	0.50 (p<0.01)	-50 to 760	237	3.4	1* (1)	Bocaina Fm, Corumba Group (Neoproterozoic)
JAR1	-3.8	-7.2	0.21 (p<0.01)	499 to 1508	318	3.2	1* (1)	Bocaina Fm Corumba Group (Neoproterozoic)
SBE3	-4.3	-8.9	0.04 (p<0.01)	-60 to 827	1710	0.5	-5.5 to -3 (2)	Urucuia Fm, Mata da Corda Group (Cretaceous)
SMT5	-4.2	-8.3	0.13 (p<0.01)	749 to 1686	575	1.6	-5.5 to -3 (2)	Urucuia Fm, Mata da Corda Group (Cretaceous)
ALHO6	-6.2	-6.6	0.57 (p<0.01)	90 to 1458	1169	1.2	-5 to 0 (3)	Guia Fm, Araras Group (Neoproterozoic)
CUR4	-7.6	-9.9	0.25 (p<0.01)	-21 to 155	252	0.7	-5 to 0(3)	Guia, Araras Group (Neoproterozoic)
DV2	-3.7	-9.2	0.35 (p<0.01)	39 to 2765	538	5.0	-9 to +10 (4)	Salitre Fm, Una Group (Neoproterozoic)
TR5	-2.9	-1.1	0.96 (p<0.01)	-57 to 76	90	1.5	-9 to +10 (4)	Salitre Fm, Uma Group (Neoproterozoic)
LD12	-3.2	-7.7	0.35 (p<0.01)	-61 to 39	122	0.8	-9 to +10 (4)	Salitre Fm, Una Group (Neoproterozoic)
TRA7	-2.8	-3.0	0.05 (p<0.01)	17 to 5507	818	6.4	0* (5)	Jandaíra Fm, Apodi Group (Cretaceous)
FN1	-2.3	-4.9	0.87 (p<0.03)	-54 to 2275	88	26.5	0* (5)	Jandaíra Fm, Apodi Group (Cretaceous)
TM0	-5.4	-9.7	0.24 (p<0.01)	-32 to 1678	471	3.6	-5 to +16 (6)	Sete Lagos Fm, Bambui Group (Neoproterozoic))
ANJOS1	-3.7	-7.2	0.09 (p<0.01)	-57 to 2927	1272	2.4	-5 t0 +2 (7)	Sete Lagoas Fm. Bambuí Group (Neoproterozoic)
BTV21a	-3.8	-8.2	0.03 (p<0.01)	196 to 9211	230	39.2	X	Botuverá Fm, Brusque Group (Neoproterozoic)
PAR3	-5.7	-8.9	0.42 (p<0.01)	-48 to 768	144	5.7	-2.2 to 5.2 (8)	Itaituba Fm Tapajos Group (Paleozoic)
PAR1	-6.6	-9.5	0.00 (p<0.44)	714 to 4812	449	9.1	-2.2 to 5.2 (8)	Itaituba Fm Tapajos Group (Paleozoic)
MV3	-1.9	-4.7	0.45 (p<0.01)	250 to 1032	537	1.4	X	Mato Virgem Fm, Natividade Group (Precambrian)
P00-H1	-13.3	-5.9	0.24 (p<0.01)	-50 to 1391	289	5.0	X	Aramachay Fm, Pucara Group (Triassic)
P09-H2	-13.0	-5.2	0.20 (p<0.01)	1099 to 7146	1272	5.7	X	Aramachay Fm, Pucara Group (Triassic)
Boto3	-9.7	-1.7	0.26 (p<0.01)	171 to 1242	256	4.0	X	Miraflores Fm, Pucara Group (Cretaceous)
Boto7	-10.8	-3.9	0.00 (p=0.6)	78 to 388	97	1.8	X	Miraflores Fm, Pucara Group (Cretaceous)
Boto10	-9.7	-3.1	0.34 (p<0.01)	543 to 1217	207	3.3	X	Miraflores Fm, Pucara Group (Cretaceous)
Boto1	-10.2	-1.2	0.41 (p<0.01)	218 to 383	20	7.9	X	Miraflores Fm, Pucara Group (Cretaceous)
PAL3	-7.1	-10.1	0.00 (p=0.2)	21 to 850	192	4.3	X	Chambara Fm, Pucara Group (Triassic_Jurassic)
PAL4	-7.1	-9.4	0.25 (p<0.01)	151 to 1536	248	5.4	X	Chambara Fm, Pucara Group (Triassic_Jurassic)

Table A1: Stalagmites and their respectively data information. (1) Novello et al. (2019); (2) Lima (2011); (3) Nogueira et al., 2006; (4) Caird et al. (2017); (5) Utida et al., 2020; (6) Alvarenga et al., 2014; (7) Caetano-Filho et al., 2019; (8) Campos (2013). (*) Site where the δ¹³C values were measured in the bedrock that hosts the cave.

Stalagmite	Coefficient of determination between growth rate & $\delta^{13}C$ (r^2)	N° of segments
JAR4	**(-) 0.21 (p=0.05)**	**18**
JAR1	(+) 0.24 (p=0.17)	9
SBE3	(+) 0.29 (p=0.12)	10
SMT5	(-) 0.35 (p=0.60)	3
ALHO6	(+) 0.03 (p=0.63)	11
CUR4	(+) 0.00 (p=0.94)	7
DV2	**(-) 0.50 (p=0.02)**	**10**
TR5	**(-) 0.75 (p<0.01)**	**7**
LD12	**(-) 0.70 (p=0.04)**	**6**
TRA7	**(-)0.20 (=0.03)**	**23**
FN1	X	3
TM0	0.00 (p=0.87)	12
ANJOS	0.00 (p=0.72)	26
BTV21a	X	3
PAR3	(-) 0.26 (p=0.24)	7
PAR1	X	3
MV3	(-) 0.46 (p=0.10)	7
P00-H1	(+) 0.55 (p=0.26)	4
P09-H2	(-) 0.35 (p=0.29)	4
Boto3	**(-) 0.94 (p=0.01)**	**8**
Boto7	X	2
Boto10	(+) 0.36 (p=0.40)	3
Boto1	X	1
PAL3	(+) 0.65 (p=0.10)	4
PAL4	(+) 0.12 (p=0.27)	11

605 **Table A2: Coefficients of determination (r^2) between growth rate, calculated based on the length interval between ages, and the mean $\delta^{13}C$ values of each interval. Correlations with confidence levels equal to or higher than 95% (p≤0.05) are shown in bold. The signal "+" and "-" denotes positive and negative slopes, respectively.**